Letter

Possible realization of the Majumdar-Ghosh point in the mineral szenicsite

Adam Berlie*
ISIS Neutron and Muon Source, Science and Technology Facilities Council, Rutherford Appleton Laboratory, Didcot, Oxfordshire, OX11 0QX, United Kingdom

Ian Terry
Department of Physics, Durham University, South Road, Durham, DH1 3LE, United Kingdom

(Received 10 February 2022; revised 1 June 2022; accepted 9 June 2022; published 22 June 2022)

The Majumder-Ghosh (MG) point is a point in parameter space for a one-dimensional (1D) frustrated system where $\alpha = J_1/J_2 = 0.5$ and the ground state is shown to be a superposition of singlet states. This leads to no magnetic order, instead the ground state is dominated by electronic dynamics, much like that of a spin liquid. Szenicsite is a natural mineral that is predicted to have isolated 1D Cu^{2+} chains and lies close to or on the MG point. In this work we use muon spin spectroscopy to demonstrate that szenicsite does not magnetically order down to 100 mK and there is an absence of a spin gap, with 1D magnetic excitations dominating. Therefore, we believe szenicsite shows the properties that would put it on the MG point and, as such, it is an interesting system for studying the properties of this quantum mechanical state.

DOI: 10.1103/PhysRevB.105.L220404

Quantum magnetism has attracted much attention over the past decade [1–5], and natural minerals [6] can provide a test-bed for particular theories or certain types of behavior. The systems in question tend to be low dimensional in nature and this often drives novel ground states [1].

Perhaps one of the simplest of the low-dimensional $S = 1/2$ systems is the case of a one-dimensional (1D) chain, where a Peierls instability causes a dimerization of spins leading to a singlet state as well as charge-ordered states [7,8]. However, when one adds in additional exchange pathways, the interactions can become complex and a degree of frustration can ensue. In the case where there is competition between a nearest-neighbor (NN) exchange interaction, J_1, and next-nearest-neighbor (NNN) exchange interaction, J_2, the frustration parameter $\alpha = J_2/J_1$ is defined. When $\alpha = 0$, the system consists of spin dimers and if $\alpha = 1$, a long-range magnetically ordered state dominates. In between, a variety of different ground states are possible.

A particular example is when $\alpha = 0.5$ and is known as the Majumdar-Ghosh model [9–12]. For an $S = 1/2$ spin chain, with NN and NNN exchange pathways at the Majumdar-Ghosh point, the ground state is solvable. This results in two states, and the ground state becomes a superposition of these two singlet states; thus long-range magnetic order is suppressed. There is also a question around whether there is an associated spin gap present.

One candidate material that is believed to be close to the Majumdar-Ghosh point is szenicsite, $Cu_3(MoO_4)(OH)_4$, a naturally occurring mineral. The chemical structure [13] is believed to be made up of 1D Cu^{2+} chains, with Cu^{2+} side chains as shown in Fig. 1. The side chains of Cu^{2+} are believed to form antiferromagetically coupled dimers so at low temperatures these are isolated from the central 1D Cu^{2+} chains. Therefore, the only exchange pathways of consequence at low temperature are the NN (J_1) and NNN (J_2) along the 1D central chain of Cu^{2+} ions [14].

The magnetic susceptibility of szenicsite follows a similar behavior to other 1D systems [14,15], where there is a broad maximum at approximately 80 K with an impurity Curie tail at low temperatures. Previous work showed that the data could be fitted by using a term to describe a 1D Heisenberg chain and antiferromagnetic (AFM) coupled dimers, with the calculated exchange energies showing agreement with theoretical calculations. From simulations of the heat capacity, the value of α for the 1D chain was estimated to be 0.45, however, this would imply that a spin gap ($\sim$4 K) would exist at low temperatures [14]. Nuclear magnetic resonance (NMR) data showed no evidence of the spin gap and that the excitations were 1D in nature, however, these experiments required one to work within the high field limit [16]. Additionally, the data did not extend down to the lowest temperatures that one needs to access to draw firm conclusions on the dynamic nature of the magnetism.

Our work utilizes muon spin spectroscopy (μSR) to probe the nature of the low-temperature magnetic state of szenicsite. We are able to demonstrate that there is no evidence of a spin gap, instead, at low temperatures, the system is in a dynamic state dominated by quantum fluctuations. This provides evidence that szenicite does in fact sit on the Majumder-Ghosh point where one expects quantum excitations to suppress any long-range order.

The szenicsite sample was mined from the Jardinera No. 1 Mine, Chile, and purchased from Crystal Classics. The szenicsite was ground to a powder and for the μSR experiment, the sample was loaded into a silver sample holder and a

*adam.berlie@stfc.ac.uk

 ©2022 American Physical Society

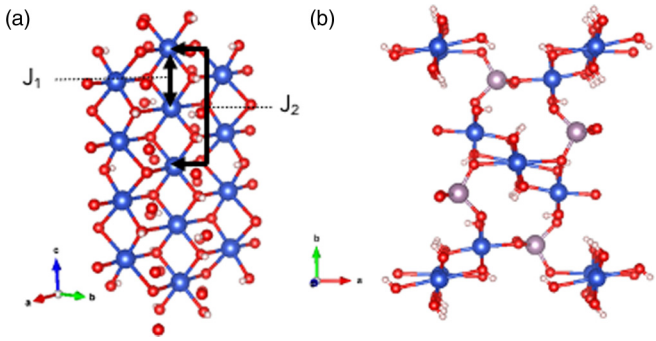

FIG. 1. Crystal structure of szenicsite; blue = copper, red = oxygen, white/cream = hydrogen, and pink = molybdenum. (a) The 1D chains run down the middle of the structure, with the Cu^{2+} dimers on the side. The intrachain exchange pathways J_1 and J_2 are illustrated. Please note that, for clarity, the Mo ions are excluded. (b) A view down the c-axis, where one can clearly see the 1D chains of the Cu^{2+}, it is the two Cu^{2+} ion either side of the central Cu^{2+} ion that form dimers along the c-axis.

small amount of dilute GE varnish in ethanol was added to create good thermal contact between crystallites. The μSR experiment was then conducted using the EMU spectrometer at the ISIS Neutron and Muon Source, UK, and using a dilution refrigerator capable of working between 50 mK and 4 K. Higher-temperature data were collected using a He-4 exchange gas cryostat. All data were analyzed using MANTID [17] and WIMDA [18].

Within a μSR experiment, spin polarized antimuons, which will be hereafter known simply as muons, are implanted within the sample, which, once thermalized, sit within an interstitial site within the crystal structure. Generally, as a first approximation, the muon will tend to locate near regions of negative charge within the unit cell. For example, within an oxide, the lone pairs on the oxygen can donate electron density to the muon, forming a dative bond.

Once thermalized, the muon then responds to the local magnetic environment (both electronic and nuclear) and is able to separate out both static and dynamic parts of the susceptibility. Following the temperature evolution of magnetic states, one can probe the nature of the magnetism within a sample and discern whether the magnetic moments order or if the system is dominated by a dynamic state due to the presence of magnetic excitations [19,20].

The muon time spectra collected from szenicsite in zero field (ZF) can be seen in Fig. 2(a). There is a remarkable similarity between all three data sets, which are offset for clarity, where the oscillation is due to the anisotropic coupling of the muon to the proton on the $[OH]^-$ groups within the crystal structure, as was demonstrated in other samples [21–23]. It is noteworthy that, although the muon may be bound to an $[OH]^-$ group, there are a few chemically distinct $[OH]^-$ groups within the crystal structure (see Fig. 1). However, it is the local anisotropic $\mu^+ \rightarrow$ H interaction that dominates the muon spin relaxation, so one cannot pick apart the different crystallographic stopping sites of the muon. The data were fit using the equation

$$G(t) = \frac{A_r}{6}\left[1 + \cos(\omega t + \phi) + 2\cos\left(\frac{\omega t}{2} + \phi\right) + 2\cos\left(\frac{3\omega t}{2} + \phi\right)\right]e^{-\lambda t} + A_B, \quad (1)$$

which describes the coupling of the muon to a single $I = 1/2$ nuclei, i.e., the proton. In Eq. (1), ω is the frequency, ϕ is the phase that accounts for the oscillations not starting at $t = 0$, A_r is the relaxing asymmetry, or simply asymmetry, λ is the muon spin relaxation rate, and A_B is the baseline, accounting for muons stopping outside of the sample, i.e., in the sample holder.

In the case of the fits within Fig. 2(a), the asymmetry was fixed at 21.5%, ϕ at 0.14 rad, and the frequency was fixed at 0.097 rad s^{-1} or 0.61 MHz, demonstrating that it is this anisotropic of coupling of the muon to the proton that dominates the depolarization of the muon spin down to the lowest temperatures. This is clear evidence that there is no magnetic order present within the sample. Generally, if bulk or local magnetic order is present, the electronic magnetism swamps any contribution from the nuclear moments. This results in either the onset of a faster precession frequency

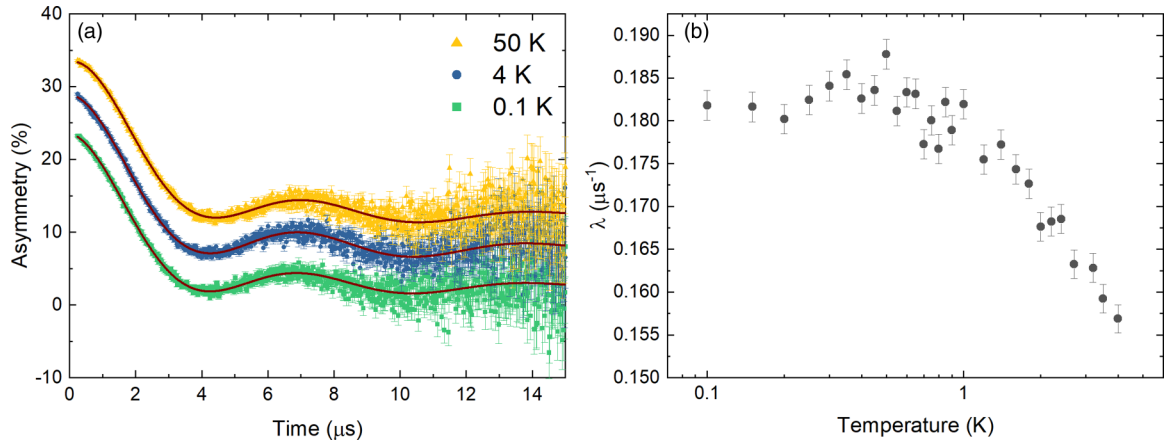

FIG. 2. Data from the zero-field μSR experiment. (a) The raw muon time spectra at different temperatures, the solid lines are fits to the data using Eq. (1). Note that the 50 K data were taken in a He-4 exchange gas cryostat. The three data sets are offset for clarity as they lie on top of each other. (b) The temperature dependence of the muon spin relaxation rate, λ.

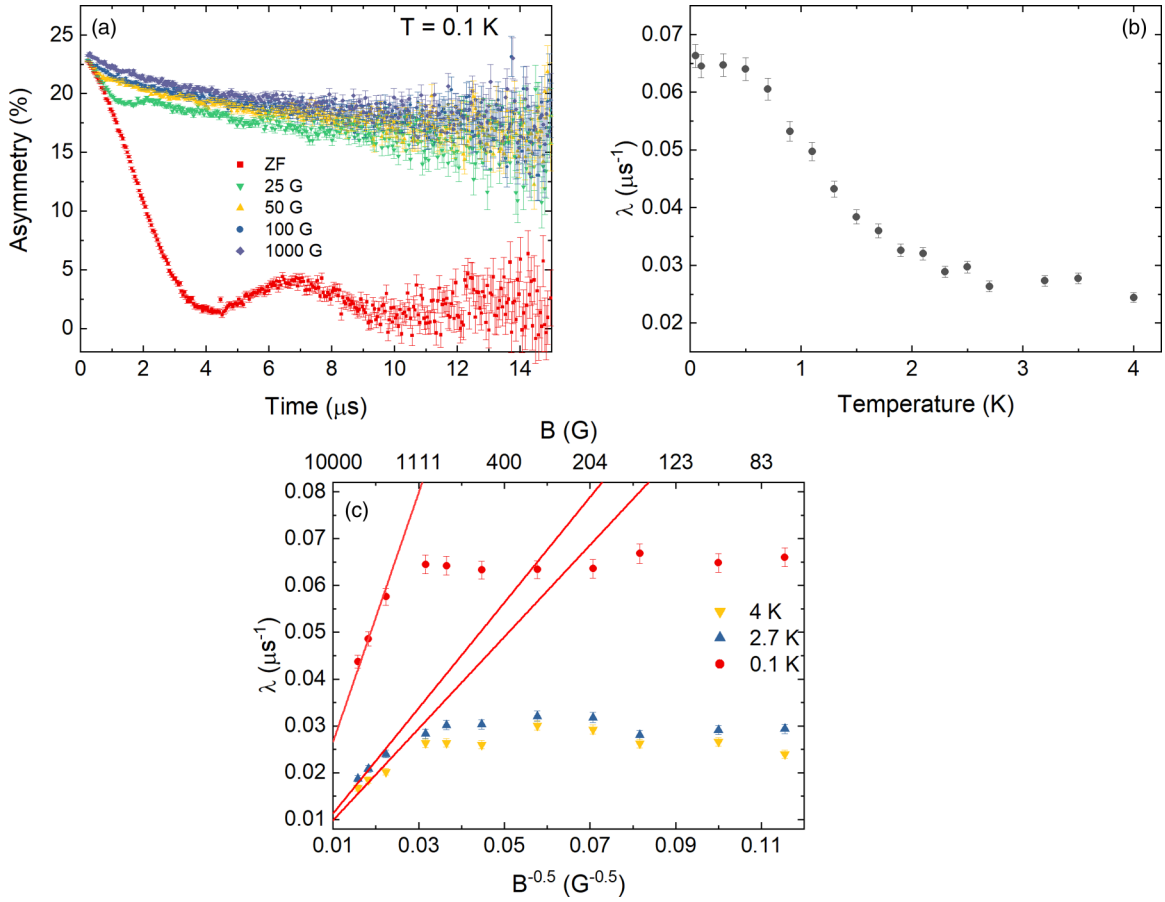

FIG. 3. (a) μSR time spectra for different longitudinal fields at 100 mK. Above 100 G LF, there is a persistent relaxation present due to the dynamics of the electronic moments within the sample. (b) The temperature dependence of the muon spin relaxation rate in a fixed LF of 1 kG. (c) The square-root field dependence of the muon spin relaxation rate at three different temperatures. At high fields, the data could be fit using the power law $\lambda \propto B^{-0.5}$, indicating the 1D nature of the spin diffusion.

that shows a temperature dependence or the appearance of a missing fraction, if the internal fields are larger than what can be measured by the technique. The only evidence of any electronic magnetism is the change in the relaxation rate, λ. The evolution of the relaxation rate is plotted in Fig. 2(b) and there is a decrease in λ as $T \rightarrow 4$ K followed by a plateau at the lowest temperatures. If the fluctuation rate of the electronic fields is faster than the experimental timescale, the influence of measurable magnetic fields will be weak. This is the likely scenario that we observe, and this is why the observed relaxation rate is small, yet still measurable.

One problem with working within ZF in this case is that the coupling of the muon to the nuclear moment on the proton dominates the depolarisation of the muon spin. To understand the behavior of the electronic moments, one can use a longitudinal field (LF), applied along the initial polarization of the muon spin, that decouples the muon ensemble from their local environment. The change in the time spectra with the application of different LFs at 100 mK can be seen in Fig. 3(a). The fact that the oscillations within the data can be damped by a moderately small field of 50 G is proof that, in ZF, the coupling of the muon to the proton is dominant. At 1 kG, there is still a relaxation present and the relaxation rate is equal to $1/T_{1\mu}$, the spin-lattice relaxation rate with respect to the muon ensemble.

By measuring the temperature dependence of the muon spin relaxation rate at 1 kG, one is able to decouple the nuclear component and is left only with the dynamic electronic component. The time spectra could be fitted using a single root-exponential relaxation

$$G(t) = A_r e^{-\sqrt{\lambda t}} + A_B, \tag{2}$$

where the parameters have the same meaning as above for Eq. (1), but in this case A_r was fixed at 11.6%. The temperature dependence of the relaxation rate, λ, can be seen in Fig. 3(b). The root-exponential physically describes the dynamics of a system with chemically distinct multiple muon stopping sites; a result of there being more then one different $[OH]^-$ environment within the crystal structure. There is a clear plateau at low temperatures and, on heating, there is a drop in λ followed by a levelling off at higher temperatures. This is evidence that, at low temperatures, there are persistent electronic fluctuations, likely quantum in nature, with a constant fluctuation rate, as has been observed in 1D chain samples before [19,20,24,25]. As the temperature is increased, the electronic moments become more dynamic in nature, with a faster fluctuation rate, which corresponds to the drop in λ. Above 2.5 K, the electronic moments are in the motionally

narrowed state and one observes a levelling off of λ as the residual relaxation dominates.

To further probe the nature of the excitations within the sample, λ was followed as a function of field [Fig. 3(c)]. At low fields, the sample is within the region where the muon-nuclear moments are being decoupled, so to probe the electronic excitations one must work generally within fields higher then ~75 G. To then quench any weak inter/intrachain spin diffusion, the system must be within the high field limit and from this the dimensionality of any dominant spin diffusion can be deduced. To this end, a plot of λ versus $B^{-0.5}$ reveals a linear region that can be fitted using a straight line. The linear dependence represents the power law $\lambda \propto B^{-0.5}$ and is a hallmark for for 1D excitations [26] where the spectral density $f(\omega) \sim \omega^{1/2}$. This matches with that previously observed using NMR for szenicsite [16]. At 4.1 K and at fields below 400 G, the knee in the data may be evidence of interchain spin diffusion, or that a particular muon site must be decoupled to observe the 1D spin diffusion. The same linear trend is also observed at 2.7 K and 100 mK, albeit with different slopes, and so there may be differences in the spin diffusion rate at the three different temperatures, which is feasible given the behavior in λ within Fig. 3(b).

The existence of 1D fluctuations are in line with the sample being dominated by the linear chains of Cu^{2+} ions. If there was the presence of singlet-triplet excitations within the dimerized side chains, one would expect to observe this within the muon spin relaxation rate as this would modulate the spin of the muon and effectively decouple it from the nuclear magnetism; this is not the case and there was no evidence of this being observed within the literature.

These data show that there is no ordered ground state. Instead, the low-temperature magnetism is dominated by 1D magnetic excitations along the Cu^{2+} chains and this would match with the behavior expected for a system lying on the Majumder-Ghosh point. However, the possibility that it is only the antiferromagnetic J_1 exchange that dominates and J_2 is negligible should also be considered as this would also result in a 1D system that cannot order. However, at these extremely low temperatures, J_2 would have to be exceptionally small, or zero energy, compared to J_1. Either way, there is strong evidence to support that this system does not order down to extremely low temperatures. This will hopefully prompt further work to provide further evidence of the quantum nature of the magnetism of this mineral.

We wish to acknowledge the ISIS Neutron and Muon Source, Science and Technology Facilities Council, for funding for samples and access to the muon spectrometer. Data can be found at [27]. We also wish to thank Francis Pratt for useful conversations regarding the data.

[1] A. Vasiliev, O. Volkova, E. Zvereva, and M. Markina, Milestones of low-D quantum magnetism, npj Quantum Mater. **3**, 18 (2018).

[2] J. Wen, S.-L. Yu, S. Li, W. Yu, and J.-X. Li, Experimental identification of quantum spin liquids, npj Quantum Mater. **4**, 12 (2019).

[3] F. Mila, Quantum spin liquids, Eur. J. Phys. **21**, 499 (2000).

[4] B. J. Powell and R. H. McKenzie, Quantum frustration in organic Mott insulators: from spin liquids to unconventional superconductors, Rep. Prog. Phys. **74**, 056501 (2011).

[5] J. R. Chamorro, T. M. McQueen, and T. T. Tran, Chemistry of quantum spin liquids, Chem. Rev. **121**, 2898 (2021).

[6] D. Inosov, Quantum magnetism in minerals, Adv. Phys. **67**, 149 (2018).

[7] M. Hase, I. Terasaki, and K. Uchinokura, Observation of The Spin-Peierls Transition in Linear Cu^{2+} (Spin-1/2) Chains in An Inorganic Compound $CuGeO_3$, Phys. Rev. Lett. **70**, 3651 (1993).

[8] H. Seo and H. Fukuyama, Charge ordering and spin gap in NaV_2O_5, J. Phys. Soc. Jpn. **67**, 2602 (1998).

[9] C. K. Majumdar and D. K. Ghosh, On next-nearest-neighbor interaction in linear chain I, J. Math. Phys. **10**, 1388 (1969).

[10] C. K. Majumdar and D. K. Ghosh, On next-nearest-neighbor interaction in linear chain, II, J. Math. Phys. **10**, 1399 (1969).

[11] W. J. Caspers, K. M. Emmett, and W. Magnus, The Majumdar-Ghosh chain. Twofold ground state and elementary excitations, J. Phys. A: Math. Gen. **17**, 2687 (1984).

[12] R. W. Chhajlany, P. Tomczak, A. Wójcik, and J. Richter, Entanglement in the Majumdar-Ghosh model, Phys. Rev. A **75**, 032340 (2007).

[13] P. C. Burns, The crystal structure of szenicsite, $Cu_3MoO_4(OH)_4$, Mineral. Mag. **62**, 461 (1998).

[14] S. Lebernegg, O. Janson, I. Rousochatzakis, S. Nishimoto, H. Rosner, and A. A. Tsirlin, Frustrated spin chain physics near the Majumdar-Ghosh point in szenicsite, Phys. Rev. B **95**, 035145 (2017).

[15] M. Fujisawa, H. Kikuchi, Y. Fujii, S. Mitsudo, A. Matsuo, and K. Kindo, New category of the frustrated quantum magnets composed of spin-1/2 triple-chains, J. Phys.: Conf. Ser. **320**, 012031 (2011).

[16] Y. Fujii, H. Kikuchi, K. Nakagawa, S. Takada, and M. Fujisawa, ^{1}H-NMR study of spin-1/2 triple-chain magnet $Cu_3(OH)_4MoO_4$, Phys. Procedia **75**, 589 (2015).

[17] O. Arnold, J. C. Bilheux, J. M. Borreguero, A. Buts, S. I. Campbell, L. Chapon, M. Doucet, N. Draper, R. Ferraz Leal, M. A. Gigg, V. E. Lynch, A. Markvardsen, D. J. Mikkelson, R. L. Mikkelson, R. Miller, K. Palmen, P. Parker, G. Passos, T. G. Perring, P. F. Peterson *et al.*, Mantid - data analysis and visualization package for neutron scattering and μ SR experiments, Nucl. Instrum. Methods Phys. Res., Sect. A **764**, 156 (2014).

[18] F. L. Pratt, WIMDA: a muon data analysis program for the Windows PC, Phys. B: Condens. Matter **289-290**, 710 (2000).

[19] *Muon Spectroscopy: An Introduction*, edited by S. J. Blundell, R. De Renzi, T. Lancaster, and F. L. Pratt (Oxford University Press, Oxford, 2021).

[20] A. D. Hillier, S. J. Blundell, I. McKenzie, I. Umegaki, L. Shu, J. A. Wright, T. Prokscha, F. Bert, K. Shimomura, A. Berlie, H. Alberto, and I. Watanabe, Muon spin spectroscopy, Nat. Rev. Methods Primers **2**, 4 (2022).

[21] J. S. Lord, S. P. Cottrell, and W. G. Williams, Muon spin relaxation in strongly coupled systems, Phys. B: Condens. Matter **289-290**, 495 (2000).

[22] E. Kermarrec, P. Mendels, F. Bert, R. H. Colman, A. S. Wills, P. Strobel, P. Bonville, A. Hillier, and A. Amato, Spin-liquid ground state in the frustrated kagome antiferromagnet $MgCu_3(OH)_6Cl_2$, Phys. Rev. B **84**, 100401(R) (2011).

[23] A. Berlie and I. Terry, Absence of quantum criticality and bulk 3D magnetism in green dioptase, EPL **120**, 47006 (2017).

[24] P. A. Goddard, J. L. Manson, J. Singleton, I. Franke, T. Lancaster, A. J. Steele, S. J. Blundell, C. Baines, F. L. Pratt, R. D. McDonald, O. E. Ayala-Valenzuela, J. F. Corbey, H. I. Southerland, P. Sengupta, and J. A. Schlueter, Dimensionality Selection in a Molecule-Based Magnet, Phys. Rev. Lett. **108**, 077208 (2012).

[25] T. Lancaster, S. J. Blundell, and F. L. Pratt, Another dimension: investigations of molecular magnetism using muon–spin relaxation, Phys. Scr. **88**, 068506 (2013).

[26] F. Xiao, J. S. Möller, T. Lancaster, R. C. Williams, F. L. Pratt, S. J. Blundell, D. Ceresoli, A. M. Barton, and J. L. Manson, Spin diffusion in the low-dimensional molecular quantum Heisenberg antiferromagnet $Cu(pyz)(NO_3)_2$ detected with implanted muons, Phys. Rev. B **91**, 144417 (2015).

[27] https://doi.org/10.5286/ISIS.E.RB2010753.